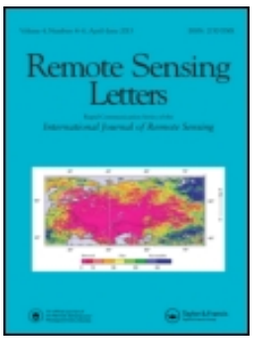

Remote Sensing Letters

ISSN: 2150-704X (Print) 2150-7058 (Online) Journal homepage: http://www.tandfonline.com/loi/trsl20

MNDISI: a multi-source composition index for impervious surface area estimation at the individual city scale

Chong Liu , Zhenfeng Shao , Min Chen & Hui Luo

To cite this article: Chong Liu , Zhenfeng Shao , Min Chen & Hui Luo (2013) MNDISI: a multi-source composition index for impervious surface area estimation at the individual city scale, Remote Sensing Letters, 4:8, 803-812, DOI: 10.1080/2150704X.2013.798710

To link to this article: https://doi.org/10.1080/2150704X.2013.798710

Remote Sensing Letters, 2013
Vol. 4, No. 8, 803–812, http://dx.doi.org/10.1080/2150704X.2013.798710

Taylor & Francis
Taylor & Francis Group

MNDISI: a multi-source composition index for impervious surface area estimation at the individual city scale

CHONG LIU, ZHENFENG SHAO*, MIN CHEN and HUI LUO
State Key Laboratory of Information Engineering in Surveying, Mapping and Remote Sensing, Wuhan University, Wuhan, China

(*Received 05 December 2012; in final form 18 April 2013*)

Impervious surface is a key indicator for monitoring urban land cover changes and human-environment interaction. Although the normalized difference impervious surface index (NDISI) has shown the potential to extract impervious surface areas (ISA) from multi-spectral imagery, it may lack robustness due to the spectral heterogeneity within urban impervious materials and confusion between other land covers. In this letter, a multi-source composition index is proposed to overcome the limitations of the original method. Three data sources: night-time light luminosity, land surface temperature and multi-spectral reflectance are integrated to create a modified NDISI (MNDISI), which aims to enhance impervious surfaces and suppress other unwanted land covers. Experimental results reveal that the MNDISI offers a stable and close relationship with ISA and is shown to be an effective index for mapping and estimating impervious surfaces in heterogeneous urban land cover environment.

1. Introduction

Impervious surfaces, defined as anthropogenic materials that water cannot infiltrate, are primarily associated with human activities (Slonecker *et al.* 2001), and have long been recognized as an important indicator in urban and environment-related studies (Weng 2012). However, it has been always difficult to estimate impervious surface areas (ISA) at the individual city scale due to the heterogeneous spectral responses within impervious materials (Moreira and Galvao 2010), the presence of mixed pixels (Small 2001) and the confusion between other land covers such as bare soil (He *et al.* 2010).

Night-time light images offer the unique ability to map human activity from space and can be a valuable indicator for urban ISA distribution (Elvidge *et al.* 2007). Although useful, the commonly used Defense Meteorological Satellite Program's (DMSP) Operational Line-scan System (OLS) (DMSP-OLS) imagery has several limitations due to its coarse pixel sizes (2.7 km) and saturation in bright urban cores. The newly onboard Visible/Infrared Imager/Radiometer Suite (VIIRS) collects night-time light free of saturation, but its spatial resolution (750 m) is still too coarse for estimating ISA at the individual city scale.

In this letter, we propose a new multi-source composition index which modifies the normalized difference impervious surface index (NDISI) developed by Xu (2010) to

*Corresponding author. Email: shaozhenfeng@whu.edu.cn

estimate urban ISA using both day-time Landsat imagery and night-time photographs taken by astronauts from the International Space Station (ISS). Both the original NDISI and the modified NDISI (MNDISI) are applied to two individual cities with different land cover conditions for performance evaluation and robustness testing.

2. Methodology

2.1 *Original NDISI*

The NDISI takes advantage of distinctive spectral response differences between impervious materials and other land covers. Most impervious surfaces tend to have high response values in the day-time thermal band (Li *et al.* 2011) and relatively low reflectance in visible, near-infrared (NIR) and middle-infrared (MIR) bands (Xu 2010). Therefore, the NDISI is developed by equation (1):

$$\mathrm{NDISI} = \frac{T_{\mathrm{LST}} - [(R_{\mathrm{VIS}} + R_{\mathrm{NIR}} + R_{\mathrm{MIR}})/3]}{T_{\mathrm{LST}} + [(R_{\mathrm{VIS}} + R_{\mathrm{NIR}} + R_{\mathrm{MIR}})/3]} \tag{1}$$

where R_{NIR} and R_{MIR} represent the reflectance of NIR and MIR bands (e.g. Thematic Mapper (TM)/Enhanced Thematic Mapper Plus (ETM+) band 4 and band 5, respectively), R_{VIS} is the reflectance from one of visible bands (e.g. TM/ETM+ band 1, 2 or 3), and T_{LST} is the land surface temperature (LST) derived from a thermal band (e.g. TM/ETM+ band 6). All index elements are re-scaled to 8 bit digital number (DN) values before its application. Nevertheless, clear water tends to have lower reflectance than impervious surfaces, and as a result, the original index may give contradictory results. To solve this problem, the modified normalized difference water index (MNDWI) (Xu 2006) can be utilized to take the place of visible band to remove the noise due to water (Xu 2010).

Although useful, there are some disadvantages to the NDISI. First, it makes the assumption that impervious materials have relatively stable spectral features. However, the spectral response of impervious surfaces inevitably varies due to aging, degradation and the use of different paints (Moreira and Galvao 2010). Figure 1 shows reflectance signatures of several urban impervious and non-impervious cover types. It is found that different impervious categories tend to have unique spectral shapes, especially in visible and NIR bands. For example, concrete road has a much stronger reflectance than other impervious surfaces in visible bands, likely generating a low NDISI value. Moreover, spectral confusions between the concrete road and bare soil in NIR bands may also give rise to uncertainty of NDISI validation. Second, NDISI is highly dependent on the LST information derived from the thermal band, which may result in relatively low estimation accuracy for some areas where urban heat island effect is not very evident (Deng and Wu 2012).

2.2 *MNDISI: the modified NDISI method*

Here we propose the MNDISI which is also based on the features of major biophysical compositions in the urban environment. In general, the process of urbanization usually leads to land cover changes and the loss of vegetation and bare soil to construct the built environment associated with intensive human activities. As a result, core urban areas with the highest density of ISA are often warmer than their rural surroundings (Zhang *et al.* 2013), with lower vegetation abundance (Small 2001, Zhang *et al.* 2013) and having greater night-time light luminosity intensity (Elvidge *et al.* 2007).

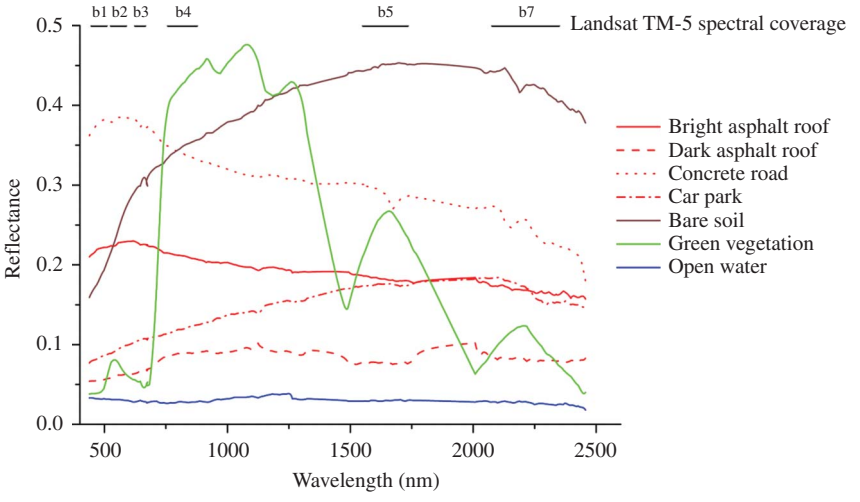

Figure 1. Reflectance signatures of several urban cover types. The original spectral measurement results are derived from Santa Barbara urban spectral library (Herold *et al.* 2003). Lines at the top of the graph indicate the spectral range of the relevant Landsat TM-5 bands (b1 = TM band 1, etc.).

For the purpose of effectively representing various impervious surfaces, the MNDISI is designed with the integrated use of different data source. We utilize both day-time LST data and night-time light luminosity to enhance the stronger responses of impervious surfaces. Also, we replace visible and NIR bands with a vegetation index (VI), which aims to enhance the diversity between some bright impervious surfaces and bare soil. The proposed MNDISI is developed by equations (2) and (3):

$$\mathrm{MNDISI} = \frac{(T_{\mathrm{LST}} - L_{\mathrm{LIT}}) - ((\mathrm{SAVI}) + R_{\mathrm{MIR}})}{(T_{\mathrm{LST}} + L_{\mathrm{LIT}}) + ((\mathrm{SAVI}) + R_{\mathrm{MIR}})} \tag{2}$$

$$\mathrm{SAVI} = \frac{(R_{\mathrm{NIR}} - R_{\mathrm{RED}})}{(R_{\mathrm{NIR}} + R_{\mathrm{RED}} + 1)} \times 1 \tag{3}$$

where L_{LIT} represents the luminosity derived from night-time light imagery, SAVI is the soil adjusted VI proposed by Huete (1988). As with the original NDISI method, here R_{RED} is the scaled reflectance of a red band (e.g. TM/ETM+ band 3) and l is a correction factor ranging from 0 for high plant densities to 1 for low plant densities. Here we adopt the recommended value by Huete (1988) $l = 0.5$ for the MNDISI validation. Choosing SAVI rather than commonly used NDVI is based on the consideration that SAVI is optimized in areas with low plant cover such as urban regions (Ray 2006).

3. Case study: implementing MNDISI at the individual city scale

3.1 *Study sites and data*

Two individual cities, Las Vegas (LV) and Los Angeles (LA) were selected as study sites (figure 2). Both LV and LA are metropolises with varieties of land covers,

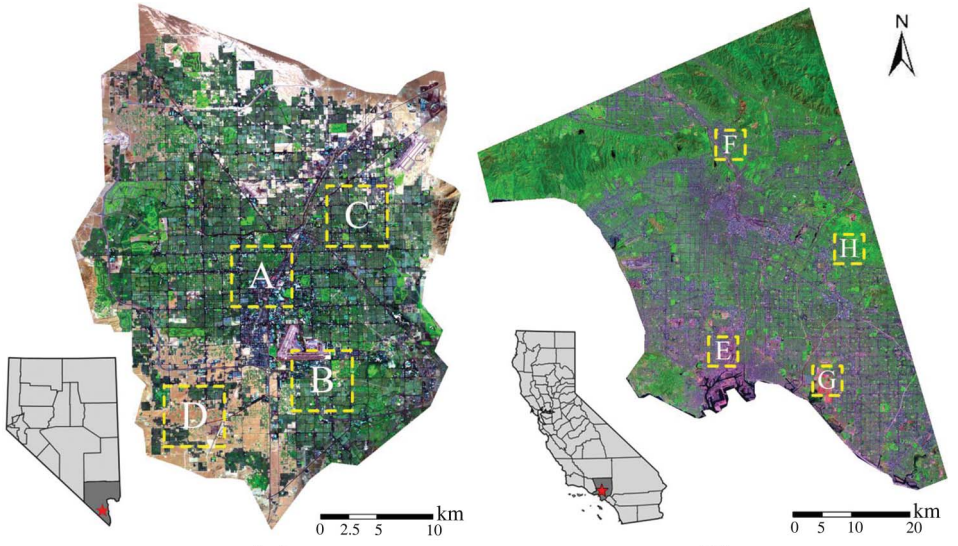

Figure 2. Landsat TM-5 false colour composites (band 7, 4 and 2 as red, green and blue) of study sites: (*a*) Las Vegas (LV, located at 36° 10′ 30″ N 115° 08′ 11″ W) in Nevada and (*b*) Los Angeles (LA, located at 34° 03′ 07″ N 118° 14′ 34″ W) in California. Note that yellow rectangular regions indicate the validation sites. Within each city, there is one site representing urban regions (site A in LV, site E in LA) and three sites representing suburban regions (site B, C and D in LV; site F, G and H in LA).

making them suitable study sites for evaluating ISA estimation methods. In addition, the climate conditions are quite different between these two cities. LV is located in arid region where vegetation coverage is much lower than LA. These differences are helpful for evaluating the robustness of the proposed method. Three remotely sensed data sources: day-time Landsat TM-5 imagery, night-time ISS photographs and high resolution ortho-imagery (HRO) aerial photographs were used and their major characteristics are summarized in table 1.

Within each city, four 6 km × 6 km sites representing various land cover types were selected to derive the reference ISA percentage data (see figure 2). Binary data (DN = 1 for ISA, DN = 0 for non-ISA) within these sites were derived based on the supervised classification results of the HRO aerial photographs. Then the number of ISA cells within each Landsat pixel area (30 m × 30 m) was calculated to generate the reference ISA percentage images of the eight sites. The final validation dataset includes 400 pixels for each city, which were randomly selected from urban and suburban sites respectively with a ratio of 1:3.

3.2 *Image pre-processing*

The raw DN values from TM multi-spectral imagery are converted to at-satellite reflectance and then normalized to 8-bit DN values. A process of water masking is applied to LA using MNDWI for removing water regions (MNDWI $\geq$ 0.4) before further analysis (water masking is not applied to LV due to its rare water presence).

Table 1. Data sources used in the letter.

Sensor	Spectral bands	Acquisition date	Source
Landsat TM-5	Six reflective bands with 30 m pixels thermal band with 120 m pixels	LV: 12 September 2010, path 39, rows 35 LA: 10 September 2010, path 41, rows 36 and 26 September 2010, path 41, rows 37	USGS Earth Explorer
Night-time ISS photograph	20 m pixels after georeferencing, with RMSE = 1.5 pixels (30 m) using HRO photographs as reference images	Images of LV and LA acquired on 30 November 2010	http://eol.jsc.nasa.gov/Coll/
HRO aerial photographs	Multiple bands (RGB) with 30 cm pixels	LV: July 2010 LA: March 2010	USGS Earth Explorer

The thermal imagery of TM band 6 is processed separately because it is a passive sensor and has a different spatial resolution. The raw DN values are first converted to at-satellite temperature, then transformed to LST (Chander *et al.* 2009) and finally normalized to 8-bit DN values. Like the original NDISI method, here we directly use coarse resolution LST for MNDISI construction because combining coarse and fine resolution images using fusion methods provides the benefit of high resolution information within the coarse resolution pixels (Xu 2010).

The original 8-bit arbitrarily scaled ISS photographs are georeferenced and rectified to universal transverse mercator (UTM) projection, WGS-84 datum using the HRO aerial photographs as reference images. A detailed description of ISS photograph pre-processing is found in Robinson *et al.* (2002). The georeferenced ISS photograph consists of three colour components, namely red, green and blue (RGB). However, a single-band image containing most of luminosity information is needed for index construction. For this purpose, a principal component analysis (PCA) is adopted and the first principal component (PC1) which typically contains about 95% luminosity information is used as the night-time light luminosity element after resampling to TM spatial resolution (30 m) and normalization to 8 bit DN values.

4. Results and discussions

Figure 3 shows the generated MNDISI results of both test cities. In particular, several subsets including various impervious land covers are extracted for validation analysis. A qualitative comparison suggests that the ISA of both cities are enhanced effectively. Both transport and building roof related impervious surfaces are depicted with a light grey to white tone in the MNDISI images, indicating high MNDISI values. On the contrary, darker pixels mainly appear in rural and city fringes, illustrating the low presence of ISA.

To further examine the effectiveness of the proposed MNDISI, comparative analyses with original NDISI are conducted within this letter. Note that for constructing NDISI, different choices can be made for the visible band, and therefore

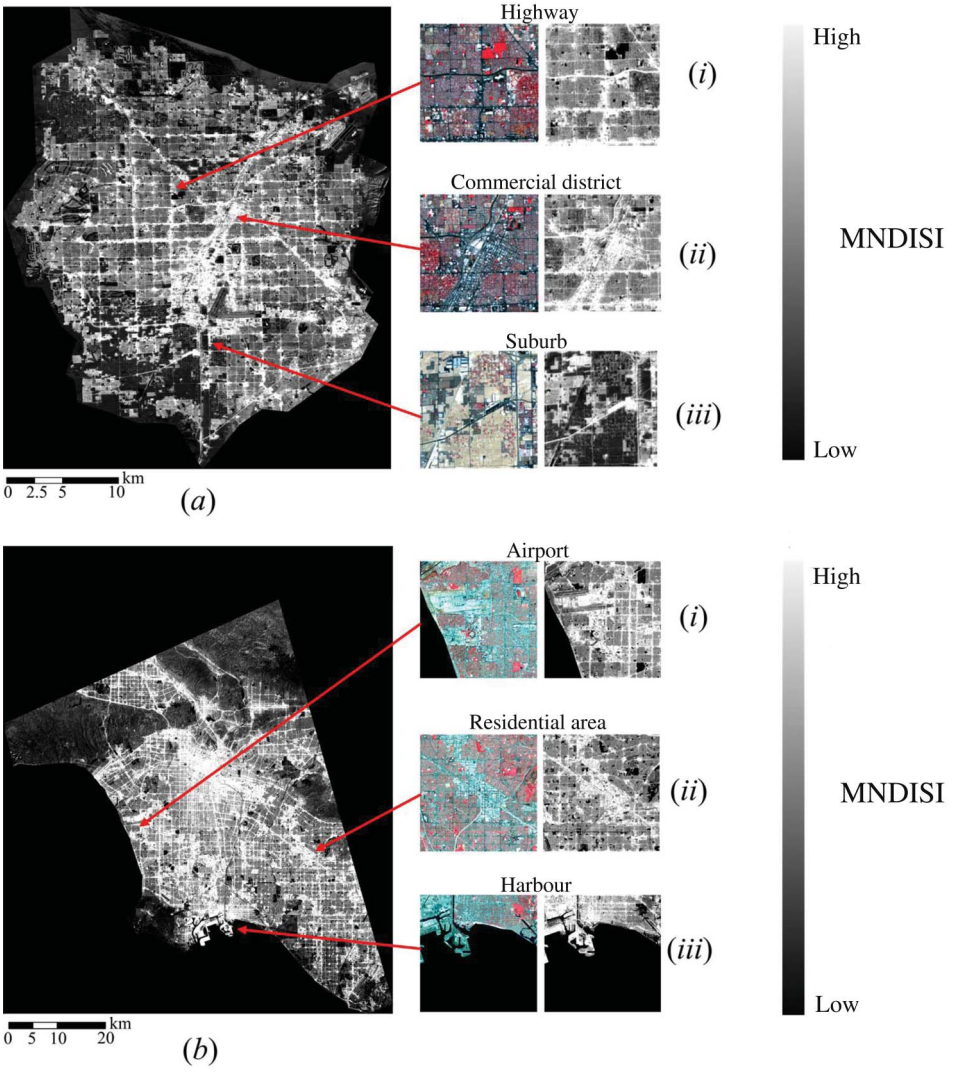

Figure 3. Grey-scale images of MNDISI results for (*a*) LV and (*b*) LA. Image chips *(i)–(iii)* illustrate the performance of MNDISI compared to standard false colour composites.

we generate four types of NDISI (using MNDWI, blue, green and red band) for comparison.

4.1 *Accuracy evaluation with reference ISA*

Since the ISA percentage is within the range 0–1, a threshold of 0 is adopted to differentiate impervious and completely non-impervious pixels. Two accuracy indicators: coefficient of determination (R^2; equation (4)) and root mean square error (RMSE; equation (5)) are employed to quantify the association between the estimated ISA results and reference data. F_i is the estimated ISA for pixel i; Y_i is the reference ISA

value for pixel i; $\overline{Y}$ is the mean value of the reference ISA samples and N is the number of pixel samples.

$$R^2 = \frac{\sum_{i=1}^{N} (F_i - \overline{Y})^2}{\sum_{i=1}^{N} (Y_i - \overline{Y})^2} \tag{4}$$

$$\text{RMSE} = \sqrt{\frac{\sum_{1}^{N} (Y_i - F_i)^2}{N}} \tag{5}$$

The results of accuracy evaluation reported in table 2 indicate slightly better accuracy performances of MNDISI for both cities with higher R^2 (0.801 for LV, 0.760 for LA) and lower RMSE (0.116 for LV, 0.117 for LA). Further, it is revealed that four types of NDISI have similar accuracy performances, illustrating their approximately equivalent effectiveness for ISA estimation as suggested by Xu (2010), except for the NDISI using MNDWI for LV, which generates a much poorer result ($R^2 = 0.147$, RMSE = 0.295) than others. This is probably due to the arid environment of LV, where the MNDWI is less useful in distinguishing impervious surfaces.

4.2 *Discrimination between impervious surfaces and other land covers*

To further examine the discrimination ability between impervious surfaces and non-impervious surfaces, we calculate index values for three major urban land covers, and a clear performance difference can be found between NDISI and MNDISI (figure 4). In particular, the MNDISI values for most vegetation and bare soil pixels are approximately equal to or less than 0 whereas impervious surfaces possess positive and higher MNDISI values. Moreover, it is observed that these histograms have narrow range, indicating a high separability level between impervious surfaces and other land covers. Although the histograms are mostly separable, minor overlaps are still found in NDISI results. One major difference between the two indices is the wider index value ranges of vegetation and bare soil by NDISI (figures 4(*a*) and (*c*)), indicating its lower separability between impervious and non-impervious surfaces. This observation is supported by the visual comparisons of indices results for two subset regions selected from validation site B (figure 5(*a*)) and F (figure 5(*b*)). It can be found that several non-impervious surface patches of NDISI results are characterized by a bright

Table 2. Accuracy evaluation results with NDISI and MNDISI in test cities.

		MNDISI		NDISI		
Sample region	Accuracy indicator		Using MNDWI	Using blue	Using green	Using red
LV	RMSE	0.116	0.295	0.191	0.196	0.202
	R^2	0.801	0.147	0.651	0.647	0.635
LA	RMSE	0.117	0.136	0.153	0.155	0.157
	R^2	0.760	0.657	0.659	0.619	0.618

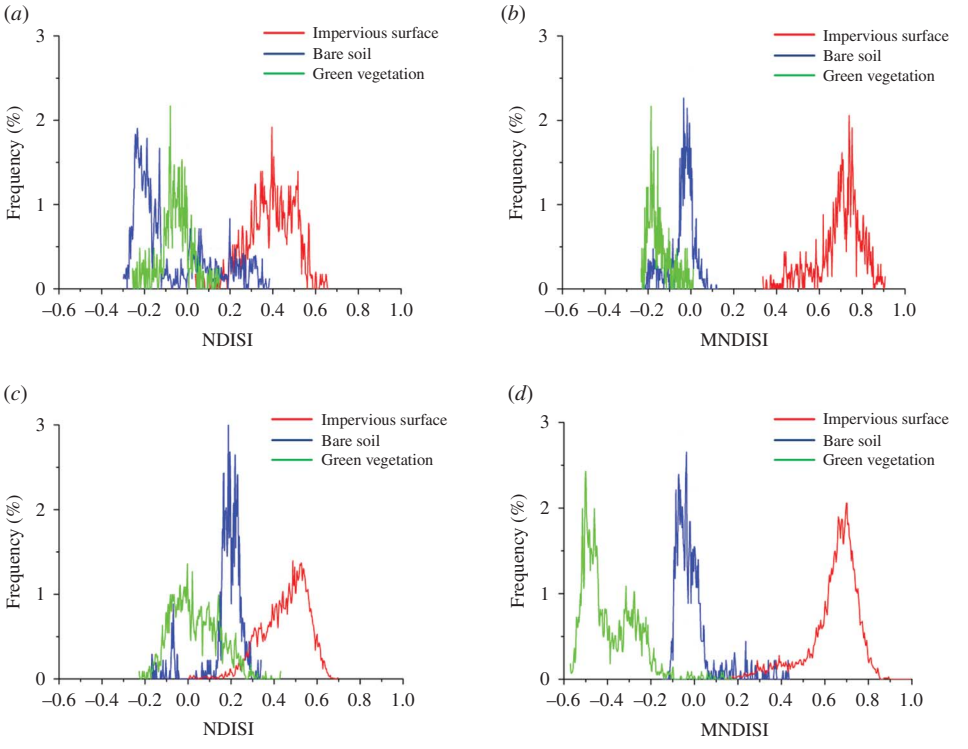

Figure 4. Histograms of NDISI (blue for visible band) and MNDISI for different land covers applied to test cities. (*a*) NDISI for LV, (*b*) MNDISI for LV, (*c*) NDISI for LA and (*d*) MNDISI for LA.

tone and therefore visually confused with impervious covers. On the contrary, these confusions are significantly reduced in the MNDISI images.

4.3 *Internal consistency of impervious surfaces*

Due to diverse spectral shapes and high within-class overall brightness variation, the accurate quantification of different kinds of impervious surfaces is critical for the validation of the proposed method. Here we investigate the internal consistency of impervious surfaces by testing the spectral discrimination index (SDI, Deng and Wu 2012) which measures the degree of cohesiveness between two categories. SDI is defined using equation (6):

$$\mathrm{SDI} = \frac{|\mu_i - \mu_j|}{\sigma_i + \sigma_j} \tag{6}$$

Where μ_i and μ_j are average index values of category i and j respectively. σ_i and σ_j are standard deviations of two categories. Obviously, for a given spectral index, SDI with a smaller value indicates better internal consistency. More specifically, two types of impervious surfaces: high albedo concrete road and low albedo car park are selected to implement SDI test for NDISI and MNDISI. Not surprisingly, the MNDISI possesses

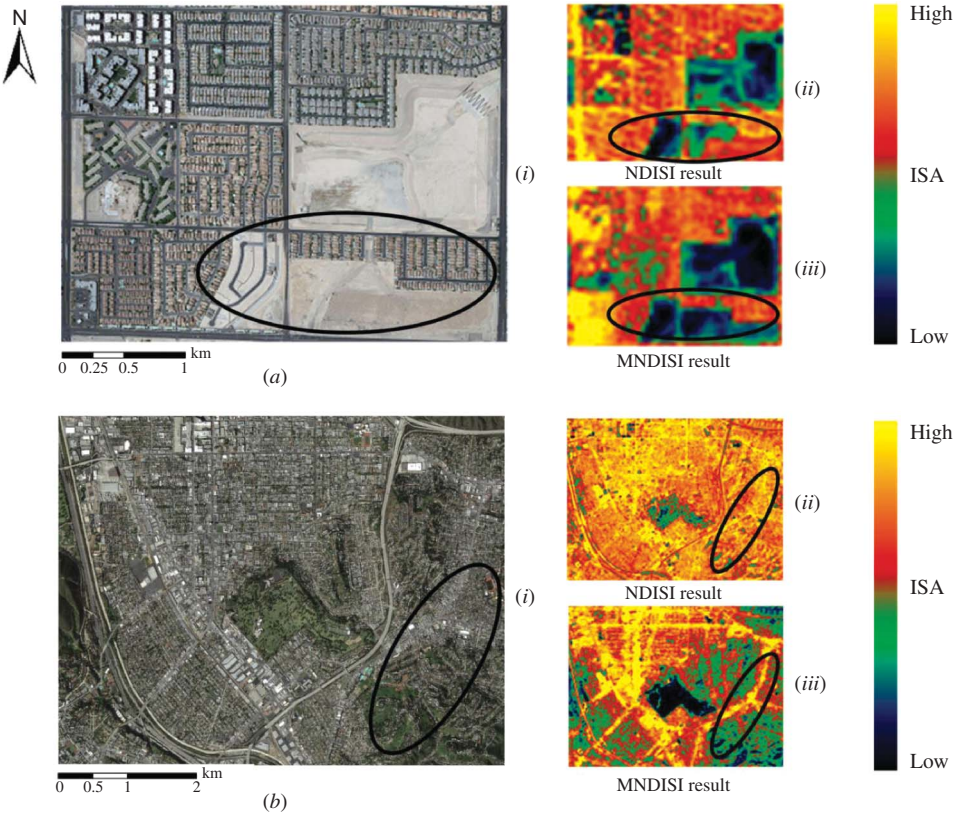

Figure 5. Comparison of the estimated ISA results by NDISI (blue for visible band) and MNDISI approaches. The main images on the left are derived from acquired HRO aerial photographs. More specifically, (*a*) is a subset of validation site B in LV covered by buildings, bare soil and sparse vegetation; (*b*) is a subset of validation site F in LA covered by dense vegetation, highways and buildings. Note that the elliptic region in each image panel indicates where the MNDISI is more accurate than NDISI.

better internal consistency in extracting both impervious surface categories. In particular, for LV the performance of MNDISI (SDI = 0.031) is slightly better than NDISI (SDI = 0.075). And this difference becomes more notable for LA. It is observed that NDISI has a much greater SDI value (SDI = 1.431) than MNDISI (SDI = 0.237).

5. Conclusions

This letter proposes a multi-source composition index which combines day-time Landsat imagery and night-time ISS photographs for measurements of urban ISA at the individual city scale. Experimental results confirm the close relationship between the index and various impervious surfaces, indicating that MNDISI can be a useful tool employed in studies of inter/intra-urban impervious surface pavement environment and their temporal variations. Moreover, the MNDISI can be developed with other data sources, such as VIIRS, whose bands span all the components of MNDISI. This provides a new potential to further implement MNDISI at different scales in the future.

Acknowledgements
The authors would like to thank Prof. Tim Warner from West Virginia University and three anonymous referees for their constructive comments.

References

Chander, G., Markham, B.L. and Helder, D.L., 2009, Summary of current radiometric calibration coefficients for Landsat MSS, TM, ETM+, and EO-1 ALI sensors. *Remote Sensing of Environment*, **113**, pp. 893–903.

Deng, C. and Wu, C., 2012, BCI: a biophysical composition index for remote sensing of urban environments. *Remote Sensing of Environment*, **127**, pp. 247–259.

Elvidge, C.D., Tuttle, B.T., Sutton, P.C., Baugh, K.E., Howard, A.T., Milesi, C., Bhaduri, B. and Nemani R., 2007, Global distribution and density of constructed impervious surfaces. *Sensors*, **7**, pp. 1962–979.

He, C., Shi, P., Xie, D. and Zhao, Y., 2010, Improving the normalized difference built-up index to map urban built-up areas using a semiautomatic segmentation approach. *Remote Sensing Letters*, **1**, pp. 295–309.

Herold, M., Gardner, M. and Roberts, D.A., 2003, Spectral resolution requirements for mapping urban areas. *IEEE Transactions on Geoscience and remote sensing*, **41**, pp. 1907–1919.

Huete, A.R., 1988, A soil-adjusted vegetation index (SAVI). *Remote Sensing of Environment*, **25**, pp. 295–309.

Li, J., Song, C., Lu, C., Zhu, F., Meng, X. and Wu, J., 2011, Impacts of landscape structure on surface urban heat islands: a case study of Shanghai, China. *Remote Sensing of Environment*, **115**, pp. 3249–3263.

Moreira, R. and Galvao, L., 2010, Variation in spectral shape of urban materials. *Remote Sensing Letters*. **1**, pp. 149–158.

Ray, T.R., 2006, *Vegetation in remote sensing FAQs in ER Mapper Applications*, pp. 85–97 (Perth: ER Mapper).

Robinson, J.A., Amsbury, D.L., Liddle, D.A. and Evans, C.A., 2002, Astronaut-acquired orbital photographs as digital data for remote sensing: spatial resolution. *International Journal of Remote Sensing*, **23**, pp. 4403–4438.

Slonecker, E.T., Jennings, D. and Garofalo, D., 2001, Remote sensing of impervious surface: a review. *Remote Sensing Reviews*, **20**, pp. 227–255.

Small, C., 2001, Estimation of urban vegetation abundance by spectral mixture analysis. *International journal of remote sensing*, **22**, pp. 1305–1334.

Weng, Q., 2012, Remote sensing of impervious surfaces in the urban areas: requirements, methods and trends. *Remote Sensing of Environment*, **117**, pp. 34–39.

Xu, H., 2006, Modification of normalized difference water index (NDWI) to enhance open water features in remotely sensed imagery. *International Journal of Remote Sensing*, **27**, pp. 3025–3033.

Xu, H., 2010, Analysis of impervious surface and its impact on urban heat environment using the normalized difference impervious surface index. *Photogrammetric Engineering and Remote Sensing*, **76**, pp. 557–565.

Zhang, Q., Schaaf, C. and Seto, K.C., 2013, The vegetation adjusted NTL urban index: a new approach to reduce saturation and increase variation in nighttime luminosity. *Remote Sensing of Environment*, **129**, pp. 32–41.